

Supporting information

Antimicrobial Peptide HPA3NT3-A2 Effectively Inhibits Biofilm Formation in Mice Infected with Drug-Resistant Bacteria

Jong-Kook Lee ^{1,2}, Loredana Mereuta³, Tudor Luchian^{3,*}, Yoonkyung Park ^{1,2,*}

¹Research Center for Proteinaceous Materials (RCPM), Chosun University, Gwangju 501-759, Korea

²Department of Biomedical Science, Chosun University, Gwangju, 501-759, Korea

³Department of Physics, Alexandru I. Cuza University, Iasi, Romania

* Corresponding authors: Yoonkyung Park and Tudor Luchian

Department of Biomedical Science, Chosun University, Gwangju, Korea.

Tel.: +82 62 230 6854

E-mail: y_k_park@chosun.ac.kr and luchian@uaic.ro

Contents

Fig. S1. Effects of HPA3NT3 and HPA3NT3-A2 on biofilms preformed on soft tissue by *Pseudomonas aeruginosa* strain 4007, a clinical isolate showing drug resistance.

Fig. S2. Scanning electron micrographs of cochlear hair cells from guinea pigs treated with HPA3NT3-A2 (256 µg/mL) or gentamicin (40 µg/mL).

Fig. S3. Effect of HPA3NT3-A2 on inflammation induced in ICR mice by *P. aeruginosa* 3241 cells (5×10^8 cfu/mL).

Fig. S4. Biofilm reduction activity of HPA3NT3-A2 peptide and Ciprofloxacin antibiotics.

Fig. S5. Effect of HPA3NT3-A2 on inflammation induced in ICR mice by *P. aeruginosa* 3241 infection.

Fig. S6. *In vivo* antimicrobial activity of HPA3NT3-A2.

Fig. S7. Effect of HPA3NT3-A2 on inflammation induced in ICR mice by *P. aeruginosa* 3241 cells (5×10^8 cfu/mL).

Fig. S8. Visualization of lung tissue from an ICR mouse with induced inflammation using a confocal laser-scanning microscope.

Fig. S9. Antimicrobial activities of HPA3NT3 and HPA3NT3-A2.

Fig. S10. Photomicrographs of lung tissue from an ICR mouse.

Fig. S11. Photomicrographs of renal tissue from an ICR mouse.

Fig. S12. Inhibition of *P. aeruginosa* 4891 cell growth in an ICR mouse.

Fig. S13. Effects of HPA3NT3 and HPA3NT3-A2 on biofilms preformed on soft contact lenses by *P. aeruginosa* 4007, a clinically isolated drug-resistant strain.

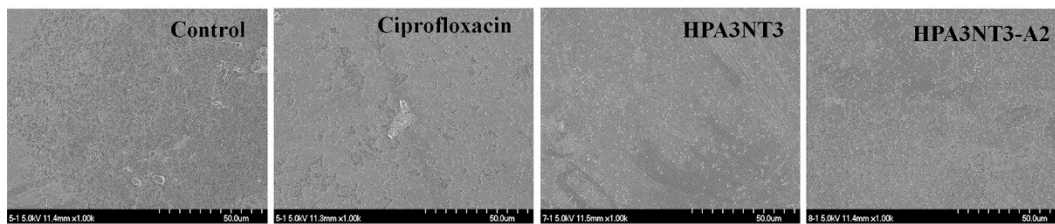


Fig. S1. Effects of HPA3NT3 and HPA3NT3-A2 on biofilms preformed on soft tissue by *Pseudomonas aeruginosa* strain 4007, a clinical isolate showing drug resistance. Biofilms were incubated for 24 h with 50 μ M HPA3NT3 or HPA3NT3-A2 or with 250 μ M ciprofloxacin. Bar = 50 μ m.

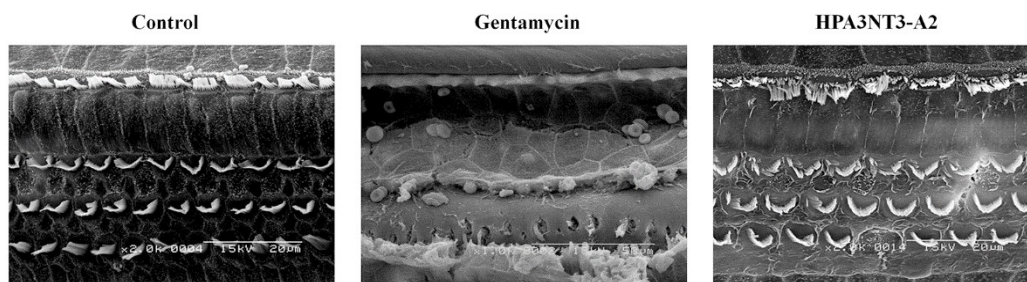


Fig. S2. Scanning electron micrographs of cochlear hair cells from guinea pigs treated with

HPA3NT3-A2 (256 $\mu\text{g}/\text{mL}$) or gentamicin (40 $\mu\text{g}/\text{mL}$). Confirmed round window (RW) in a guinea pig inner ear 7 days after gel foam treatment using 20 μL or gentamicin or HPA3NT3-A2. Bar = 20 μm .

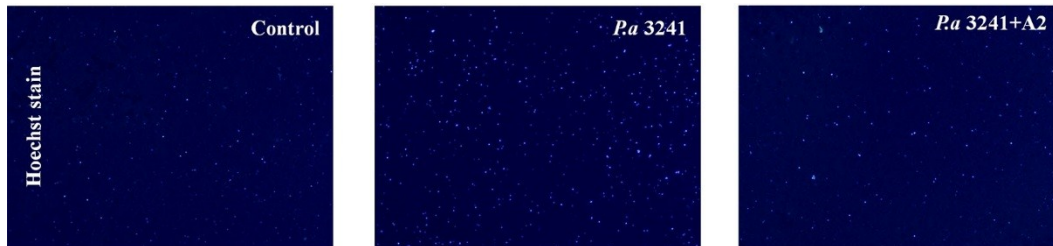


Fig. S3. Effect of HPA3NT3-A2 on inflammation induced in ICR mice by *P. aeruginosa* 3241 cells (5×10^8 cfu/mL). Shown are white blood cells (WBCs) from whole blood collected from mice administered *P. aeruginosa* 3241 (5×10^8 cfu/mL) with or without HPA3NT3-A2 (1 mg/kg). The WBCs were stained with Hoechst dye (0.25 mg/mL) and counted under a microscope. Bar = 20 μm .

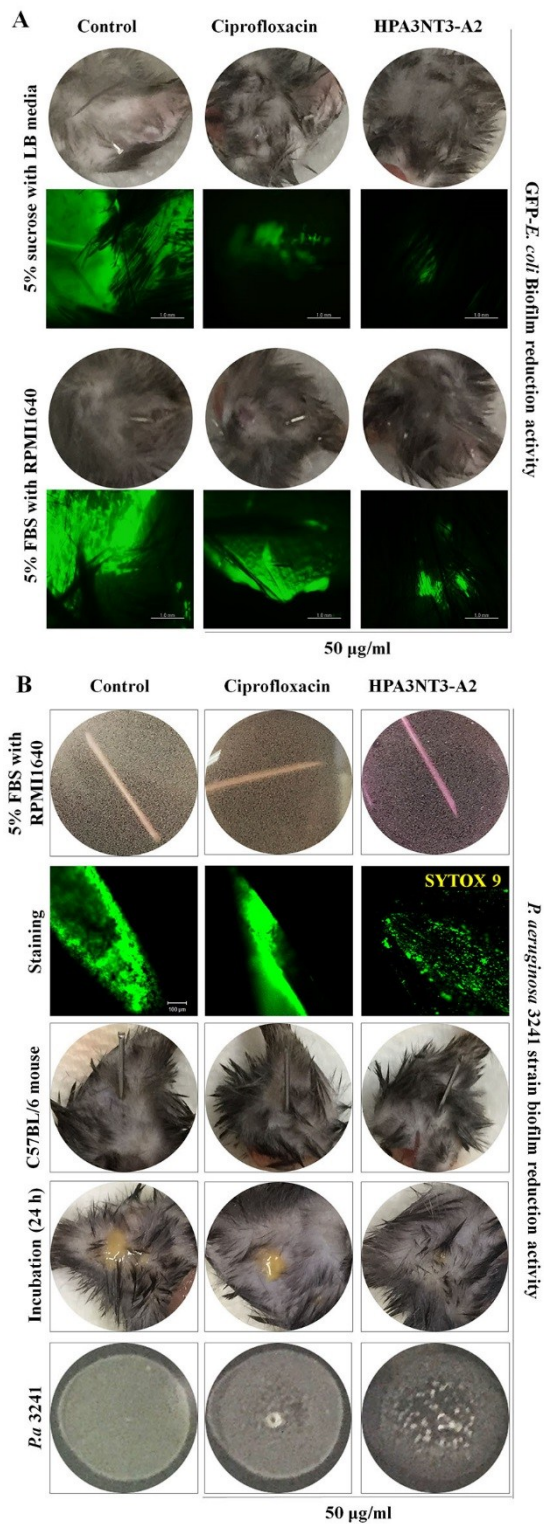


Fig. S4. Biofilm reduction activity of HPA3NT3-A2 peptide and Ciprofloxacin antibiotics. HPA3NT3-A2 peptide and ciprofloxacin antibiotics biofilm activity reduction on biofilms formed on injection needles using GFP-*E. coli* (1×10^8 cfu/mL). The biofilm-formed injection needle was treated with 50 µg/mL HPA3NT3-A2 peptide and/or ciprofloxacin antibiotics, and incubated for 24 h.

Thereafter, the injection needle was injected into the skin of C57BL/6 mice, incubated for 12 h, and evaluated using fluorescence microscopy. Bar = 1.0 mm (A). Biofilm preformed on the injection needle by *P. aeruginosa* (1×10^8 cfu/mL) strain 3241 was treated with 50 μ g/mL HPA3NT3-A2 peptide and ciprofloxacin antibiotics, incubated for 24 h, stained with CYTOX 9 dye, and evaluated using fluorescence microscopy. Bar = 1.0 mm. In addition, the injection needle was injected into the skin of C57BL/6 mice skin and incubated for 24 h. The skin was intensely ground, spread on NB (Nutrient Broth) agar plates (0.5 % NaCl), and incubated for 24 h (B).

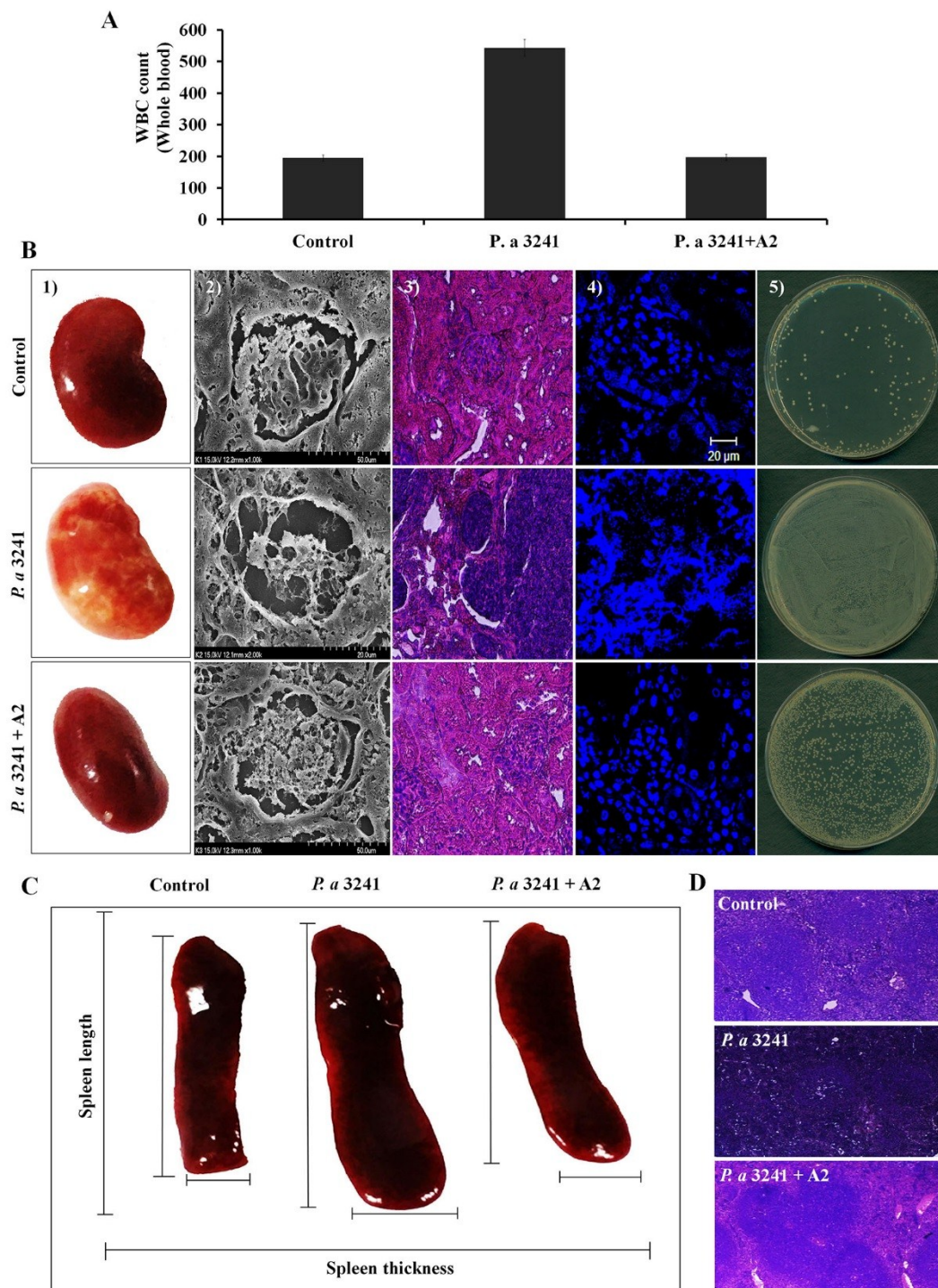


Fig. S5. Effect of HPA3NT3-A2 on inflammation induced in ICR mice by *P. aeruginosa* 3241 infection. After extraction of whole blood from mice left untreated (Control) or inoculated with *P. aeruginosa* 3241 cells (intravenous injection; 5×10^8 cfu/mL) with or without HPA3NT3-A2 peptide (1 mg/kg), while blood cells (WBCs) were stained with Hoechst dye and evaluated by fluorescence

microscopy (A). The effect of HPA3NT3-A2 peptide on inflammation in kidney tissues from ICR mice induced by *P. aeruginosa* 3241 infection (B). Whole kidney tissues showing induced inflammation in the presence or absence of HPA3NT3-A2 (1 mg/kg) (1). Electron micrographs showing induced inflammation detected in the presence or absence of HPA3NT3-A2 peptide. Bar = 10 μ m (2). Fluorescence and confocal micrographs of whole kidney tissue from ICR mice with induced inflammation. Photomicrographs of H&E (3) and DAPI stained sections of renal tissue. Bar = 20 μ m (4). Whole kidney homogenates on NB agar plates (0.5% NaCl) after incubation for 20 h at 37°C (5): upper panel, from a control mouse; middle panel, from a mouse injected with *P. aeruginosa*; lower panel, from a mouse injected with *P. aeruginosa* and HPA3NT3-A2. The effect of HPA3NT3-A2 on induced inflammation in splenic tissues from ICR mice. Shown are the length and thickness (C) of whole spleens and H&E staining of splenic tissue (D). All values represent the mean \pm SEM of three individual experiments ($P < 0.05$, one-way ANOVA).

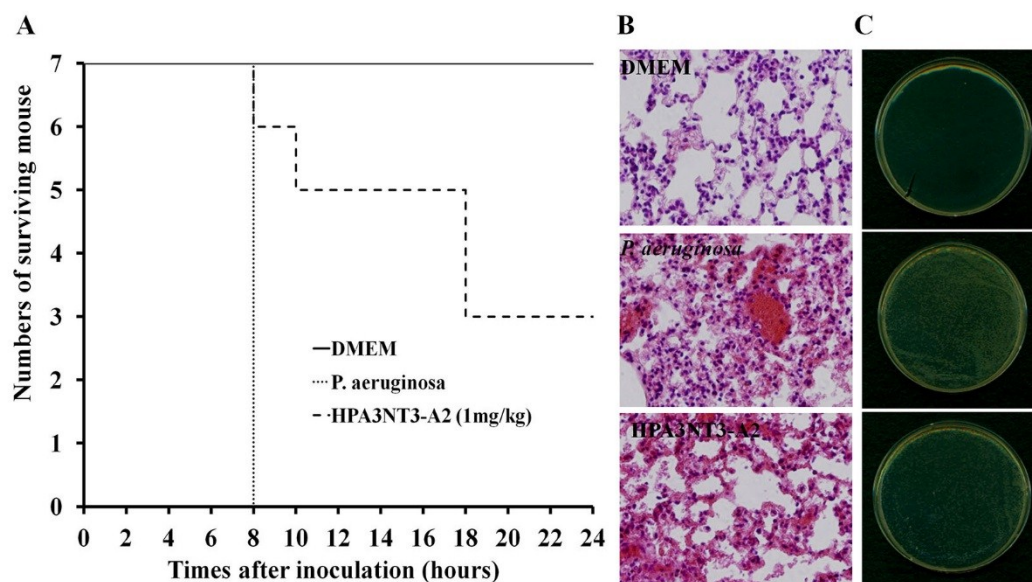


Fig. S6. *In vivo* antimicrobial activity of HPA3NT3-A2. The survival rates among *P. aeruginosa* 4007 (5×10^8 cfu/mL)-infected ICR mice after a single injection of HPA3NT3-A2 (1 mg/kg) administered 1 h post-infection (A). Histological appearance of lungs from infected mice with and without HPA3NT3-A2 treatment (H&E stain, 40 \times) (B). Lung homogenates from ICR mice were spread on

NB agar plates and incubated for 12 h at 37°C (C).

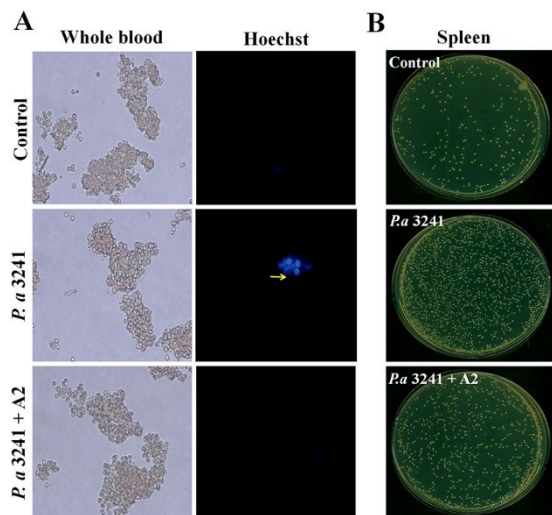


Fig. S7. Effect of HPA3NT3-A2 on inflammation induced in ICR mice by *P. aeruginosa* 3241 cells (5×10^8 cfu/mL). Shown are white blood cells (WBCs) from whole blood collected from mice administered *P. aeruginosa* 3241 (5×10^8 cfu/mL) with or without HPA3NT3-A2 (1 mg/kg). The WBCs were stained with Hoechst dye (0.25 mg/mL), and then evaluated by fluorescence microscopy. Bar = 40 μ m (A). Colony formation from whole liver homogenates (0.5% NaCl) spread on NB agar plates after incubation for 20 h at 37°C (B).

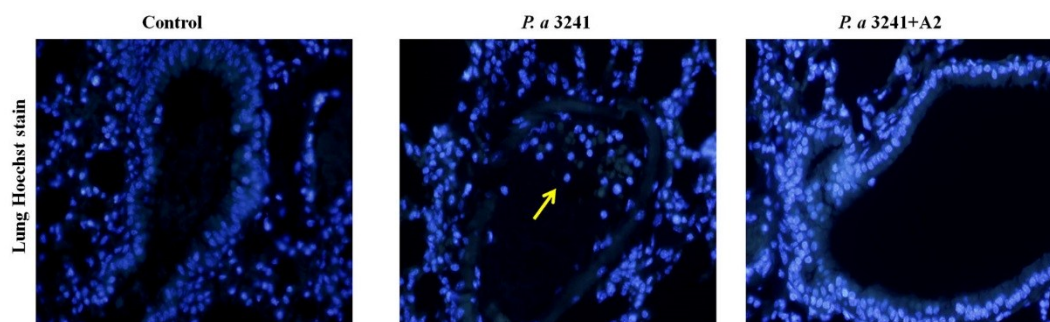


Fig. S8. Visualization of lung tissue from an ICR mouse with induced inflammation using a confocal laser-scanning microscope. All tissues were sectioned at 4 μ m using a microtome and stained with

DAPI. Bar = 20 μ m.

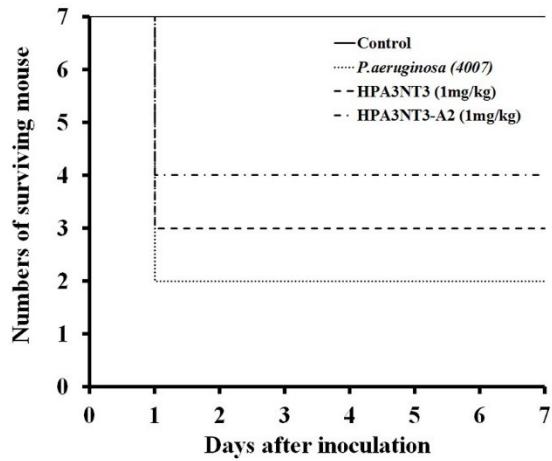


Fig. S9. Antimicrobial activities of HPA3NT3 and HPA3NT3-A2. The survival rates among ICR mice infected with *P. aeruginosa* strain 4007 (5×10^8 cfu/mL) after treatment with HPA3NT3 or HPA3NT3-A2 (1 mg/kg) 1 h post-infection.

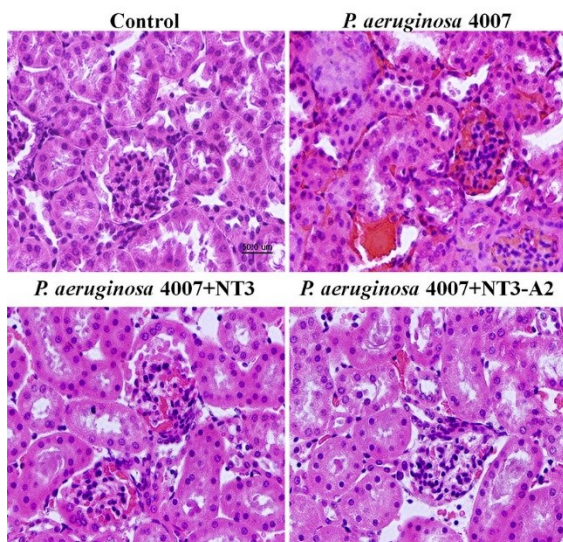


Fig. S10. Photomicrographs of lung tissue from an ICR mouse. Lung tissue was sectioned at 4 μ m using a microtome and stained with H&E. Bar = 20 μ m.

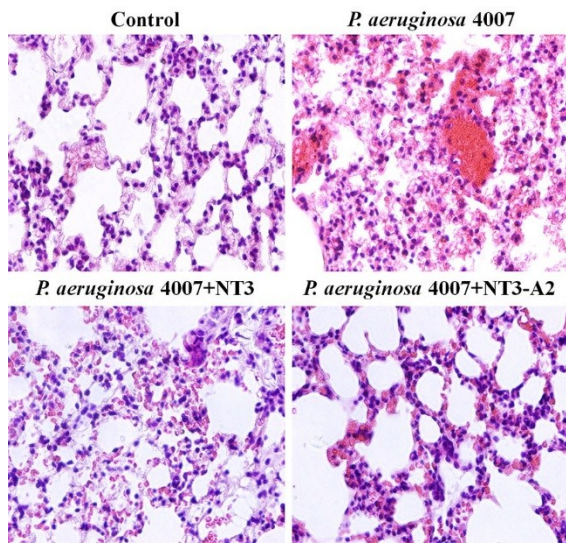


Fig. S11. Photomicrographs of renal tissue from an ICR mouse. Lung tissue was sectioned at 4 μm using a microtome and stained with H&E. Bar = 20 μm .

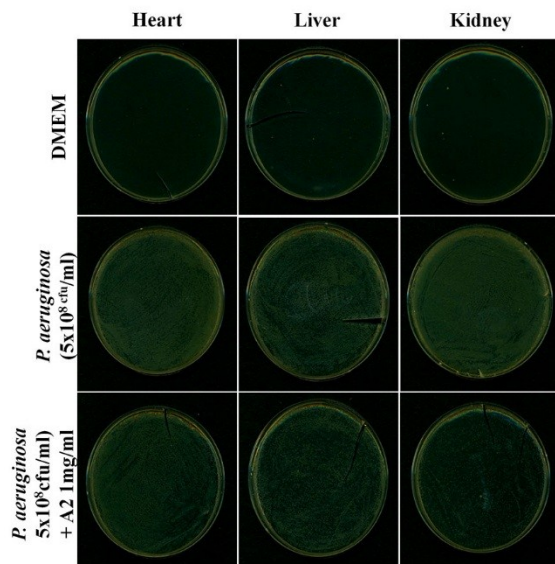


Fig. S12. Inhibition of *P. aeruginosa* 4891 cell growth in an ICR mouse. HPA3NT3-A2 was used to treat the infection. Heart, liver, and kidney tissues were extracted, homogenized, spread on agar plates, and incubated for 12 h at 37°C.

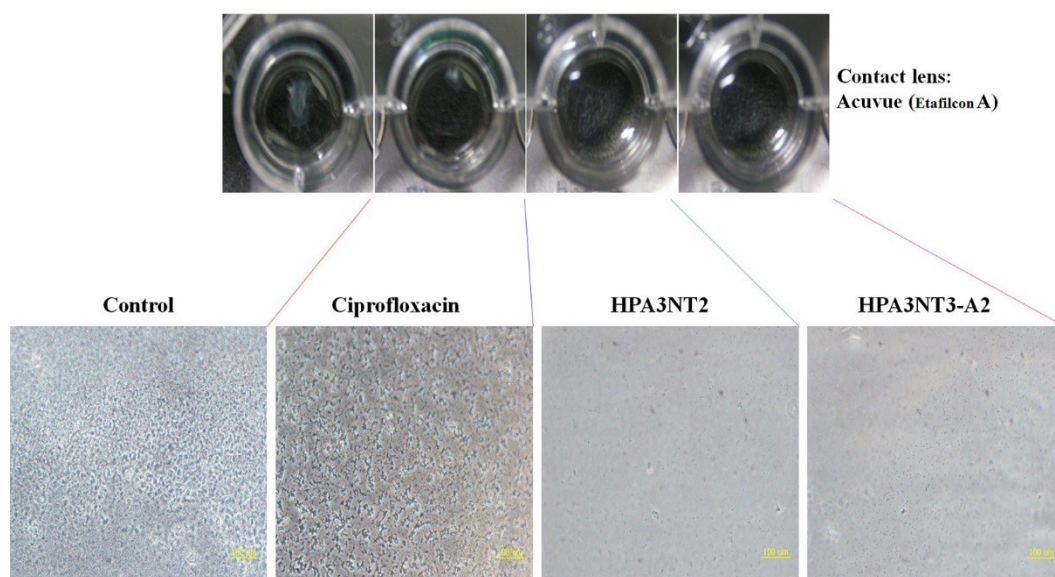


Fig. S13. Effects of HPA3NT3 and HPA3NT3-A2 on biofilms preformed on soft contact lenses by *P. aeruginosa* 4007, a clinically isolated drug-resistant strain. The lenses were incubated for 24 h with 32 μM HPA3NT3 or HPA3NT3-A2 or with 500 μM ciprofloxacin.